Comparison of discrete fiber and asymptotic homogenization methods for modeling deformations of fiber-reinforced materials

Petr E. Zakharov, Petr V. Sivtsev

Ammosov North-Eastern Federal University, 58, Belinskogo, 677000 Yakutsk, Russia

E-mail: zapetch@gmail.com

Abstract.

The main issue in a numerical simulation of fiber-reinforced materials deformation is high computational complexity. Exact resolution of fibers thickness leads to a huge number of degrees of freedom. In this work, we compare discrete fiber and asymptotic homogenization methods for modeling deformations. The discrete fiber method considers fibers as one-dimensional lines and the asymptotic homogenization method averages elasticity coefficients. We investigate the accuracy of these methods for a large range of models and approximation parameters.

1. Introduction

Fiber-reinforced materials are recommended as most of the strongest composite materials, e.g. concrete with basalt-polypropylene fiber inclusions [1]. Another example of fiber-reinforced material is load-bearing concrete structure reinforced with basalt plastic or steel [2, 3]. One of the popular trends in development technologies is related to the production of basalt fiber and composite materials based on it.

In numerical modeling of the stress-strain state of fiber-reinforced materials, the main issue is related to a huge quantity of the mesh cells to take into account. There are numerical methods, which reduce the initial problem to a more simplified problem, e.g. homogenization or multiscale methods [4, 5]. The discrete fiber method, which is similar to the discrete fracture method [6, 7] in porous media simulation, can be used for fiber-reinforced material simulation as well.

In this work, we compare two approaches of fiber-reinforced material modeling: the discrete fiber and the asymptotic homogenization methods. In the discrete fiber method (DFM) we assume that fibers are one-dimensional and we take account only stress-strain state along the fiber length. In this simplification, we can reduce the number of mesh cells, i.e. degrees of freedom. The asymptotic homogenization method (AHM) [9–12] is convenient for the domain containing a large amount of repeated subdomains. With AHM, we compute averaged elastic tensor and solve the problem on a coarse mesh. These two approaches have advantages and, in some cases, one of them can be more convenient than the other. We make a numerical investigation of the cases, in which the methods show better accuracy. Numerical implementations are performed using finite element package FEniCS [8].

2. Problem Statement

We consider a problem in the unit square $\Omega = (0,1)^2$, where Ω_1 is the main material and $\Omega_2 = \cup_{i=1}^{K} \phi_i$ is the subdomain of K fiber inclusions. The stress-strain state of fiber-reinforced material is described by the following equation for the displacement $\boldsymbol{u} = (u_1, u_2)$

$$\nabla \cdot \boldsymbol{\sigma} = \boldsymbol{f}, \quad \boldsymbol{x} \in \Omega, \tag{1}$$

where $\boldsymbol{\sigma} = \boldsymbol{C}\boldsymbol{\varepsilon}$ is the stress tensor, $\boldsymbol{C}$ is the elastic tensor and $\boldsymbol{\varepsilon}$ is the strain tensor, $\boldsymbol{f}$ is the force source. To describe the numerical methods we use Voight notation

$$\boldsymbol{\sigma} = \begin{pmatrix} \sigma_{11} \\ \sigma_{22} \\ \sigma_{12} \end{pmatrix}, \quad \boldsymbol{C} = \begin{pmatrix} C_{1111} & C_{1122} & C_{1112} \\ C_{2211} & C_{2222} & C_{2212} \\ C_{1211} & C_{1222} & C_{1212} \end{pmatrix}, \quad \boldsymbol{\varepsilon} = \begin{pmatrix} \varepsilon_{11} \\ \varepsilon_{22} \\ \varepsilon_{12} \end{pmatrix} = \begin{pmatrix} \frac{\partial u_1}{\partial x_1} \\ \frac{\partial u_2}{\partial x_2} \\ \frac{\partial u_2}{\partial x_1} + \frac{\partial u_1}{\partial x_2} \end{pmatrix}.$$

We assume that the main material and fibers are isotropic. Then the elastic tensor can be expressed by Lame parameters λ_i, μ_i depending on the subdomain

$$\boldsymbol{C}_i = \begin{pmatrix} \lambda_i + 2\mu_i & \lambda_i & 0 \\ \lambda_i & \lambda_i + 2\mu_i & 0 \\ 0 & 0 & \mu_i \end{pmatrix}, \quad \boldsymbol{x} \in \Omega_i, \quad i = 1, 2.$$

Lame parameters are expressed by Young modulus E_i and Poisson coefficient ν_i

$$\lambda_i = \frac{E_i\, \nu_i}{(1+\nu_i)(1-2\nu_i)}, \quad \mu_i = \frac{E_i}{2(1+\nu_i)}, \quad \boldsymbol{x} \in \Omega_i, \quad i = 1, 2.$$

Equation (1) is supplemented with boundary conditions. On the left border Γ_L, we fix the displacement using Dirichlet condition

$$\boldsymbol{u} = (0, 0), \quad \boldsymbol{x} \in \Gamma_L.$$

And on the right border Γ_R, we apply the force using Neumann condition

$$\boldsymbol{\sigma_n} = \boldsymbol{g}, \quad \boldsymbol{x} \in \Gamma_R.$$

where $\boldsymbol{\sigma_n} = \boldsymbol{\sigma}\, \boldsymbol{n}$ and $\boldsymbol{n}$ is the normal vector to the border.

3. Finite Element Mehtod

As a reference solution, we use the solution of finite element approximation where fibers are taken into account in full size. We get the following variational statement for our problem: find the function $\boldsymbol{u} \in V$, which satisfies $a(\boldsymbol{u}, \boldsymbol{v}) = L(\boldsymbol{v}), \forall \boldsymbol{v} \in \widehat{V}$, where $a(\boldsymbol{u}, \boldsymbol{v})$ is the bilinear form, $L(\boldsymbol{v})$ is the linear form

$$a(\boldsymbol{u}, \boldsymbol{v}) = \int_{\Omega_1} \boldsymbol{C}_1\, \boldsymbol{\varepsilon}(\boldsymbol{u}) : \boldsymbol{\varepsilon}(\boldsymbol{v})\, \mathrm{d}\boldsymbol{x} + \int_{\Omega_2} \boldsymbol{C}_2\, \boldsymbol{\varepsilon}(\boldsymbol{u}) : \boldsymbol{\varepsilon}(\boldsymbol{v})\, \mathrm{d}\boldsymbol{x}, \tag{2}$$

$$L(\boldsymbol{v}) = \int_{\Omega} \boldsymbol{f}\, \boldsymbol{v}\, \mathrm{d}\boldsymbol{x} + \int_{\Gamma_R} \boldsymbol{g}\, \boldsymbol{v}\, \mathrm{d}\boldsymbol{s}, \tag{3}$$

and V, $\widehat{V}$ are the trial and test function spaces

$$V = \widehat{V} = \{\boldsymbol{v} \in H^1(\Omega) : \boldsymbol{v} = (0,0), \boldsymbol{x} \in \Gamma_L\},$$

$H^1(\Omega)$ is the Sobolev function space. We use first order Lagrange elements as finite elements.

4. Discrete Fiber Method

In the discrete fiber method similar to the discrete fracture method, we consider fibers as one-dimensional. We represent subdomain Ω_2 by set of lines and denote by $\Gamma_2 = \cup_{i=1}^{K} \gamma_i$, where γ_i is the fiber line. In this case, we get the following bilinear and linear forms for our problem

$$a(\boldsymbol{u}, \boldsymbol{v}) = \int_{\Omega} \boldsymbol{C}_1\, \boldsymbol{\varepsilon}(\boldsymbol{u}) : \boldsymbol{\varepsilon}(\boldsymbol{v})\, \mathrm{d}\boldsymbol{x} + \int_{\Gamma_2} d\,(\lambda_2 + 2\mu_2 - \lambda_1 - 2\mu_1)(\nabla \boldsymbol{u}_{\boldsymbol{\tau}}\, \boldsymbol{\tau})(\nabla \boldsymbol{v}_{\boldsymbol{\tau}}\, \boldsymbol{\tau})\mathrm{d}\boldsymbol{s},$$

$$L(\boldsymbol{v}) = \int_{\Omega} \boldsymbol{f}\, \boldsymbol{v}\, \mathrm{d}\boldsymbol{x} + \int_{\Gamma_R} \boldsymbol{g}\, \boldsymbol{v}\, \mathrm{d}\boldsymbol{x},$$

where d is the thickness of fibers, $\boldsymbol{u}_{\boldsymbol{\tau}} = \boldsymbol{u}\, \boldsymbol{\tau}$ and $\boldsymbol{\tau}$ is the tangent vector to a fiber line. In this approximation, we take into account only compression and tension of fibers along to fiber line and neglect other effects. Function spaces and finite elements are the same as in the finite element approximation.

5. Asymptotic Homogenization Method

We assume that our composite material can be divided into equal squares with fibers on the same locations. Then we can compute an effective elastic tensor using well known asymptotic homogenization method. Let denote an average value of function ψ by following notation

$$\langle \psi \rangle = \frac{\int_{\omega} \psi\, \mathrm{d}\boldsymbol{x}}{\int_{\omega} \mathrm{d}\boldsymbol{x}},$$

where ω is a periodic domain. Thus, an average stress tensor can be expressed by

$$\langle \boldsymbol{\sigma} \rangle = \langle \boldsymbol{C}\, \boldsymbol{\varepsilon} \rangle = \boldsymbol{C}^{*} \langle \boldsymbol{\varepsilon} \rangle,$$

where $\boldsymbol{C}^{*}$ is the effective elastic tensor. To compute corresponding components of the effecitve elastic tensor, we consider three problems in the periodic domain ω with the following force sources:

(i) $C^{*}_{ij11} = \langle \sigma_{ij} \rangle, \quad ij = 11, 22, 12$, from $\boldsymbol{f} = -\nabla \cdot \boldsymbol{C}\, \boldsymbol{\varepsilon}((x_1, 0))$,
(ii) $C^{*}_{ij22} = \langle \sigma_{ij} \rangle, \quad ij = 11, 22, 12$, from $\boldsymbol{f} = -\nabla \cdot \boldsymbol{C}\, \boldsymbol{\varepsilon}((0, x_2))$,
(iii) $C^{*}_{ij12} = \langle \sigma_{ij} \rangle, \quad ij = 11, 22, 12$, from $\boldsymbol{f} = -\nabla \cdot \boldsymbol{C}\, \boldsymbol{\varepsilon}((x_2/2, x_1/2))$.

To ensure the uniqueness of the solution, we fix displacement to $(0, 0)$ in the middle point of the domain ω. To solve the periodic problems, we use the same variational forms (2), (3) as in the finite element approximation. We change only function spaces

$$V = \widehat{V} = \{\boldsymbol{v} \in H^1(\omega) : \boldsymbol{v}(\boldsymbol{x}) = \boldsymbol{v}(\boldsymbol{x} + \boldsymbol{p}), \boldsymbol{p} = (0, l), (l, 0)\},$$

where l is the side of square domain ω.

After computing the average elastic tensor, we find the coarse solution using the next variational statement: find the function $\boldsymbol{u} \in V$, which satisfies $a(\boldsymbol{u}, \boldsymbol{v}) = L(\boldsymbol{v}), \forall \boldsymbol{v} \in \widehat{V}$, where

$$a(\boldsymbol{u}, \boldsymbol{v}) = \int_{\omega} \boldsymbol{C}^{*}\, \boldsymbol{\varepsilon}(\boldsymbol{u}) : \boldsymbol{\varepsilon}(\boldsymbol{v})\, \mathrm{d}\boldsymbol{x}, \quad L(\boldsymbol{v}) = \int_{\Omega} \boldsymbol{f}\, \boldsymbol{v} \mathrm{d}\, \boldsymbol{x} + \int_{\Gamma_R} \boldsymbol{g}\, \boldsymbol{v}\, \mathrm{d}\boldsymbol{s}.$$

Function spaces and finite elements are the same as in the finite element approximation. We compare only a coarse solution and do not compute a higher order solution of the asymptotic homogenization method. In this case, for a coarse solution, we can use the same number unknowns as in periodic problems, i.e. a finer mesh. Also, it gives less difference with a reference solution.

6. Numerical Experiments

For numerical comparison, we consider simple square domain Ω with $n \times n$ equal subdomains ω. Each subdomain ω contains uniformly distributed $k = K/n^2$ fibers with size $l \times d$, where $l = \frac{1}{2n}$ is the lenght and d is the thickness. In fig. 1 we show domain with $n \times n = 4 \times 4$ subdomains ω with $k = 2$ fibers. We consider two variants of subdomains: ω_{ahm} with full size fibers and ω_{dfm} with one-dimensional fibers. To discretize domain Ω, we use a uniform triangular mesh with grid step h. The grid size of subdomain ω is $n \times n$ less than the grid size of domain Ω.

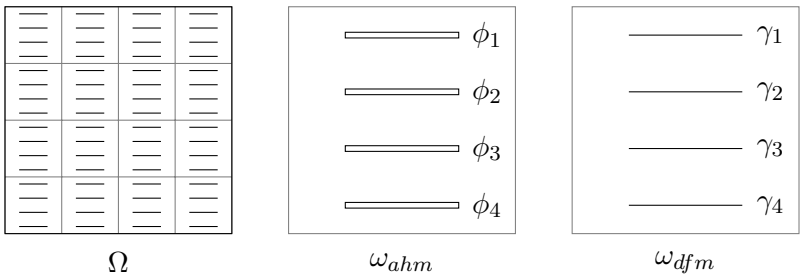

Figure 1. Problem domain Ω, subdomain ω_{ahm} for AHM and ω_{dfm} for DFM

In our numerical investigation we use the following model parameters: $E_1 = 2 \cdot 10^{10}, E_2 = \alpha E_1, \nu_1 = \nu_2 = 0.3, \boldsymbol{g} = (0, -10^5)$, where α is the ratio of Young modulus.

Let denote two norms of relative errors by

$$\epsilon^i_{L_\infty} = \frac{\|\boldsymbol{u}^i - \boldsymbol{u}^{fem}\|_{L_\infty}}{\|\boldsymbol{u}^{fem}\|_{L_\infty}}, \quad \epsilon^i_{L_2} = \frac{\|\boldsymbol{u}^i - \boldsymbol{u}^{fem}\|_{L_2}}{\|\boldsymbol{u}^{fem}\|_{L_2}}, \quad i = dfm, ahm,$$

where $\boldsymbol{u}^{fem}$ is the FEM reference solution, $\boldsymbol{u}^{dfm}$ is the DFM solution and $\boldsymbol{u}^{ahm}$ is the AHM solution. We compare DFM and AHM implementations in 5 tests. In each test we vary one of this parameters: k, d, α, n, h, and all other parameters are fixed.

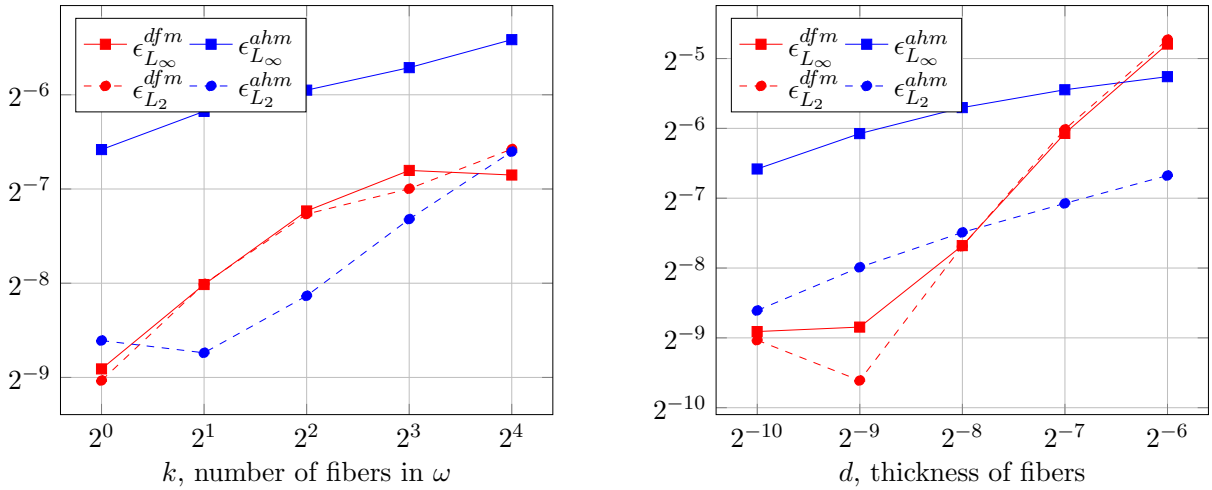

Figure 2. Errors depending on number and thickness of fibers

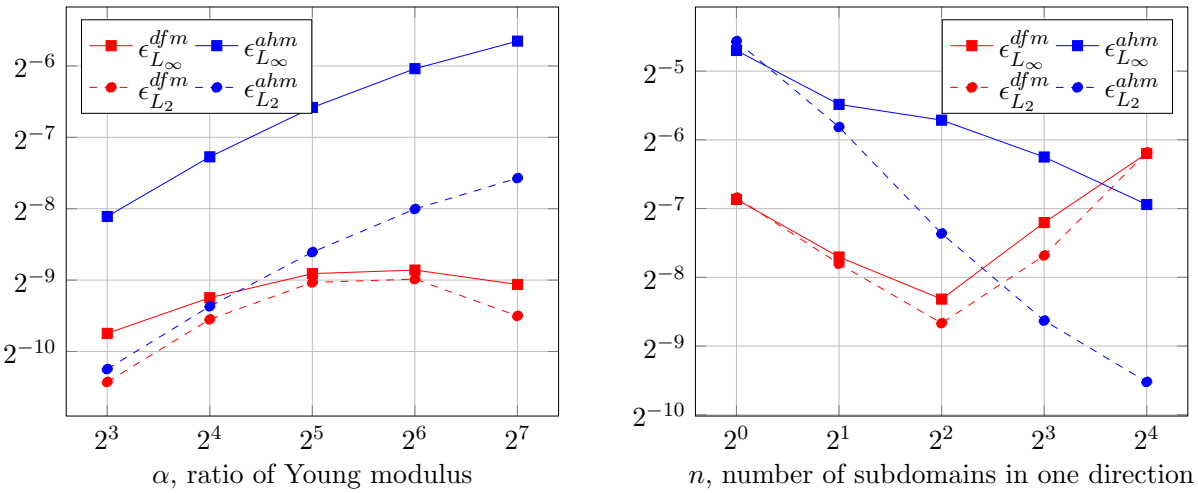

Figure 3. Errors depending on ration of Young modulus and number of subdomains

In fig. 2 we show a comparison of relative errors for different number k and thickness d of fibers. For these calculations, we fix the next parameters: $n = 4, d = 1/1024, \alpha = 32, h = 1/2048$. As we can see, both relative errors of DFM are almost the same. And the AHM L_∞ norm of error is much higher than L_2 due to the localization of the error near fibers. Both methods show that the relative errors increase with a number of fibers. For all cases k, the error L_2 norms are similar and differ less than 2 times. And DFM error L_∞ norm is better more than 2 times comparing to AHM. DFM solution is more sensitive to the thickness of fibers d and the relative error grows faster than AHM error. But for fibers with a small thickness, i.e. with a high ratio of length and thickness, DFM gives a more precise solution than AHM.

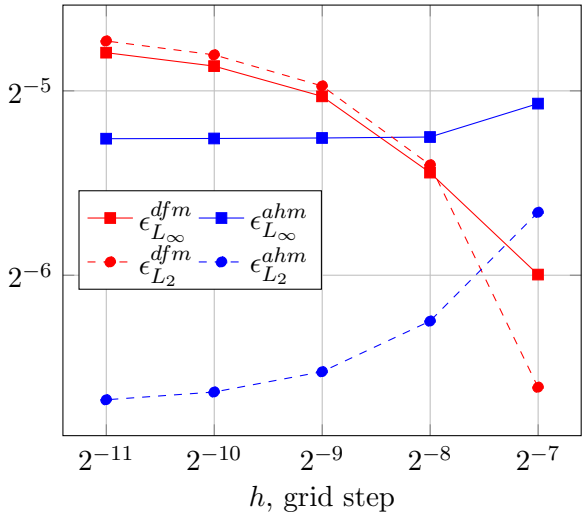

Figure 4. Error depending on grid step

In the next two tests, we investigate dependence on α ration of Young modulus and n number of subdomains. Calculated relative errros are plotted in fig. 3. For simulations with α variation, we use the following parameters: $n = 4, d = 1/1024, k = 1, h = 1/2048$ and for n variation: $d = 1/1024, k = 1, h = 1/(128\,n)$. DFM solution shows better accuracy for high α ratio of

Young modulus and the error is almost constant for different α. AHM error increses with α. However, AHM error decreases on increasing n number of subdomains. For large n AHM accuracy is better than DFM and DFM error increases linearly with number of subdomains.

The last test is conducted to compare errors depending on h grid step, see fig. 4. To neglect FEM error, we solve the reference solution on the finest grid with step $h = 1/2048$. Due to the variation of grid steps, we choose the large thickness of fibers $d = 1/64$, i.e length and thickness ratio $l/d = 8$, and DFM error is larger than AHM error. Other parameters: $n = 4, k = 1, \alpha = 32$. For the fine grids, the errors are close to methods of approximation errors and are almost constant. AHM error increases for the coarse grids and this corresponds to the theory. DFM error decreases for the coarse grids due to opposite signs of FEM (in DFM) and DFM errors, which neglect each other.

7. Conclusion

We have numerically investigated two approaches of deformation modeling of fiber-reinforced materials. DFM showed better accuracy for a large ration of Young modulus between main material and fibers comparing to AHM. Moreover, DFM is more convenient for thick fibers, which have a large ration of length and thickness. AHM solution is better for domains containing a large number of equal subdomains. And one of the most important advantages of DFM is the use of more coarse meshes, where fibers are represented as lines, which reduces degrees of freedom.

References

[1] Smarzewski, P.: Influence of basalt-polypropylene fibres on fracture properties of high performance concrete. Composite Structures 209, 23-33 (2019)

[2] Sivtseva, A.V., Sivtsev, P.V.: Numerical Simulation of Deformations of Basalt Roving. International Conference on Finite Difference Methods, 501–508 (2018).

[3] Kolesov A. E. et al.: Numerical Analysis of Reinforced Concrete Deep Beams. International Conference on Numerical Analysis and Its Applications. – Springer, Cham, 414-421 (2016).

[4] Zakharov, P.E., Sivtsev, P.V.: Numerical calculation of the effective coefficient in the problem of linear elasticity of a composite material. Mathematical notes of NEFU 24.2, 75-84 (2017).

[5] Stepanov, S.P., Vasilyeva, M.V., Vasil'ev, V.I.: Generalized multiscale discontinuous Galerkin method for solving the heat problem with phase change. Journal of Computational and Applied Mathematics 340, 645-652 (2018).

[6] Vasil'ev V. I. et al.: Numerical solution of a fluid filtration problem in a fractured medium by using the domain decomposition method. Journal of Applied and Industrial Mathematics 12(4), 785-796 (2018).

[7] Akkutlu I. Y. et al.: Multiscale model reduction for shale gas transport in a coupled discrete fracture and dual-continuum porous media. Journal of Natural Gas Science and Engineering 48, 65-76 (2017).

[8] Logg, A., Mardal, K.A., Wells, G.N.: Automated solution of differential equations by the finite element method. Springer (2012).

[9] Pinho-da-Cruz J., Oliveira J. A., Teixeira-Dias F. Asymptotic homogenisation in linear elasticity. Part I: Mathematical formulation and finite element modelling. Computational Materials Science 45(4), 1073-1080 (2009)

[10] Oliveira J. A., Pinho-da-Cruz J., Teixeira-Dias F. Asymptotic homogenisation in linear elasticity. Part II: Finite element procedures and multiscale applications. Computational Materials Science 45(4), 1081-1096 (2009)

[11] Pellegrino C., Galvanetto U., Schrefler B. A. Numerical homogenization of periodic composite materials with non-linear material components. International Journal for Numerical Methods in Engineering 46(10), 1609-1637 (1999)

[12] Yuan Z., Fish J. Toward realization of computational homogenization in practice. International Journal for Numerical Methods in Engineering 73(3), 361-380 (2008)